






FULL PAPER

Dual inhibition of carbonic anhydrases VA and VII by silychristin and isosilybin A from *Silybum marianum*: A potential antiobesity strategy

Emanuele Liborio Citriniti¹ | Roberta Rocca^{1,2,3}  | Giosuè Costa^{1,2}  |
Gioele Renzi⁴  | Fabrizio Carta⁴  | Claudiu T. Supuran⁴ | Stefano Alcaro^{1,2,3}  |
Francesco Ortuso^{1,2}

¹Dipartimento di Scienze della Salute, Università "Magna Græcia" di Catanzaro, Catanzaro, Italy

²Net4Science S.r.l., Università "Magna Græcia" di Catanzaro, Catanzaro, Italy

³Associazione CRISEA—Centro di Ricerca e Servizi Avanzati per l'Innovazione Rurale, Catanzaro, Italy

⁴NEUROFARBA Department, Sezione di Scienze Farmaceutiche, University of Florence, Florence, Italy

Correspondence

Roberta Rocca, Dipartimento di Scienze della Salute, Università "Magna Græcia" di Catanzaro, Viale Europa, 88100 Catanzaro, Italy.

Email: rocca@unicz.it

Funding information

PON "Ricerca e Innovazione" 2014-2020, grant number No. 26* code DOT13C5773-4

Abstract

Obesity is a global health crisis linked to chronic diseases like cardiovascular disease and type 2 diabetes. Its prevalence, even in low-income countries, highlights the failure of traditional interventions. Safer pharmacological treatments are urgently needed, as many existing antiobesity drugs have been withdrawn due to severe side effects, leaving a critical therapeutic gap. A promising target in this context is human carbonic anhydrase V (hCA V), a mitochondrial enzyme that plays a key role in glucose homeostasis. Inhibiting hCA V has been shown to reduce lipogenesis and improve metabolic conditions. Natural plant extracts, such as silymarin from milk thistle, have demonstrated potential in managing obesity-related metabolic syndromes by lowering triglycerides, reducing cholesterol levels, and improving liver function. Our computational studies have identified active compounds in silymarin that effectively inhibit hCA V, shedding light on a potential mechanism for its antiobesity effects. Building on these findings, our research further reveals that these compounds also inhibit carbonic anhydrase VII (hCA VII), enhancing their therapeutic potential. This dual inhibitory action addresses both metabolic dysregulation and oxidative stress. Notably, the antioxidant properties of hCA VII provide additional protection against obesity-related complications by mitigating oxidative stress, a key contributor to the development of metabolic syndrome.

KEYWORDS

docking, dual inhibition, hCAs, milk thistle, obesity

1 | INTRODUCTION

Obesity is a pressing global public health concern that impacts people worldwide. It significantly contributes to chronic illnesses, including cardiovascular disease,^[1] certain types of cancer,^[2] nonalcoholic fatty

liver disease,^[3] and type 2 diabetes mellitus.^[4] The global issue of obesity has reached epidemic proportions, with its prevalence tripling in several European nations and affecting a significant portion of the populace. Once considered problems primarily affecting affluent nations, obesity and its associated health risks are now spreading

This is an open access article under the terms of the [Creative Commons Attribution](https://creativecommons.org/licenses/by/4.0/) License, which permits use, distribution and reproduction in any medium, provided the original work is properly cited.

© 2025 The Author(s). *Archiv der Pharmazie* published by Wiley-VCH GmbH on behalf of Deutsche Pharmazeutische Gesellschaft.

rapidly to lower income countries, posing an alarming global threat.^[5,6] Obesity is a severe health condition that is challenging to treat with lifestyle and behavioral changes alone. While these adjustments can help alleviate some symptoms, they are often not sufficient for long-term effectiveness.^[7] Adding pharmacological and surgical interventions to the treatment plan can lead to more significant results. However, many antiobesity medications have been developed and approved in the past, but they were later withdrawn due to severe side effects experienced by a significant number of patients. This lack of safe and effective long-term options has created a growing interest in discovering new antiobesity drugs.^[5]

Scientists are actively investigating potential targets for the development of antiobesity medications. One of the most promising targets identified is carbonic anhydrase V (*hCA V*), a mitochondrial enzyme directly involved in glucose homeostasis. With its favorable side effect profile, *hCA V* stands out as an attractive candidate for the development of new antiobesity therapies.^[8,9] The human AC VA/B isoforms (*hCA VA* and *VB*) are important from a biological perspective because the mitochondrial membrane is impermeable to bicarbonate ions and only permeable to CO_2 . Moreover, there are no carriers for bicarbonate ions belonging to the SLC4A family. This means that *de novo* synthesis of bicarbonate within this compartment is essential for making substrates available to pyruvate carboxylase in the process of gluconeogenesis and lipogenesis, and carbamoyl phosphate synthase I in the process of ureagenesis in the liver. Thus, inhibiting *hCA VA* and *VB* could lead to a significant decrease in citrate levels, promoting a reduction in lipogenic phenomena. These isoenzymes may also be involved in insulin secretion and neuromodulation. Therefore, there is increasing interest in AC V as a potential target for different compounds with pharmacological activity.^[10,11]

In the last decade, extensive research has been conducted on plant extracts and their phytochemical constituents to evaluate their potential effectiveness in combating obesity.^[11,12] Ethnopharmacology is an indispensable field for the discovery of new drugs and systematic screening of both pharmacological and phytochemical aspects.^[13,14] Indeed, plants found in the wild are known to contain valuable plant secondary metabolites like polyphenols and terpenoids that have potential use as nutraceuticals, particularly in functional foods. Research on edible wild plants, using both *in vitro* and *in vivo* models, has revealed their capacity to contain active compounds that offer health benefits. Among the various plants of the Mediterranean basin, *Silybum marianum* (L.), commonly known as milk thistle (MT), is very interesting for its beneficial effects on metabolic syndrome. It is an annual/biennial weed and a trusted herbal remedy for liver and biliary tract ailments. *S. marianum* is also known for its numerous health benefits, including antioxidant, lipid-lowering, antihypertensive, anti-diabetic, antiatherosclerotic, antiobesity, and hepatoprotective effects, making it an effective treatment for metabolic syndrome.^[15]

The extract of *S. marianum*, commonly known as Silymarin, is primarily used to treat liver-related disorders. This substance exhibits a variety of reported activities, including antioxidant, antifibrotic, regenerative, choleric, hepatoprotective, immunostimulatory, and anti-inflammatory effects. Silymarin is a standardized dry extract

derived from the seeds of the *S. marianum* plant, predominantly composed of flavonolignans, which make up about 70%–80% of its total weight.^[16] Additionally, a combination of flavonoids, including polymerized and oxidized polyphenolic compounds, can be observed. Flavonolignans are a relatively limited subgroup of compounds where the flavonoid part of the molecule is fused with a lignan. Silybin, isosilybin (A and B), silydianin, and silychristin are the primary flavonolignans found in silymarin, and they are the most biologically active compounds within the extract, despite the identification of unconventional flavolignans.^[17] Although numerous studies have detailed the analytical separation and quantification of silymarin components in extracts from various plant parts, seasons, and geographic locations, there is currently no comprehensive comparison of flavonolignan profiles in different silymarin preparations.^[18–20] Studies have shown that the extract of Silymarin can reduce triglyceride levels in patients with nonalcoholic fatty liver disease (NAFLD) who consumed daily doses of 7.1 g of MT for 3 months as a source of silymarin (210 mg per day).^[21] An *in vivo* study on obese mice with metabolic syndrome and consequent type 2 diabetes mellitus and cardiovascular pathologies such as hypertension showed that the intake of silymarin reduced total body weight without affecting lean body weight. It also reduced serum levels of total cholesterol, triglycerides, and low-density lipoproteins (LDL) while improving insulin resistance in obese mice. Furthermore, the extract improved evident liver damage and hepatic steatosis in the group fed with a high-fat diet (HFD). Silymarin enhanced the degree of hepatic steatosis and inflammation in liver tissue, reducing serum Alanine Aminotransferase and Aspartate Aminotransferase levels. The results suggest that silymarin could effectively inhibit HFD-induced hepatic steatosis and improve liver function. Therefore, the extract of Silymarin obtained from the MT plant could represent an effective aid in the prevention and treatment of metabolic syndromes related to obesity and related disorders.^[22]

In light of the above, we have decided to use computational methods to explore the most biologically active compounds found in MT extract. We aim to evaluate the efficacy of these compounds as *hCA VA* inhibitors by examining how they interact with the three-dimensional (3D) structure of carbonic anhydrase isoforms found in the Protein Data Bank (PDB). To achieve this, we used a structure-based approach that involved docking and molecular dynamics (MDs) simulations. After identifying the top compounds from the *in silico* analysis, we conducted enzymatic assays to validate the results. This study revealed the molecular mechanism behind the antiobesity effect of two active compounds from *S. marianum* (L.) by demonstrating their interaction and inhibition of *hCA VA*.^[15]

2 | RESULTS AND DISCUSSION

2.1 | Molecular docking

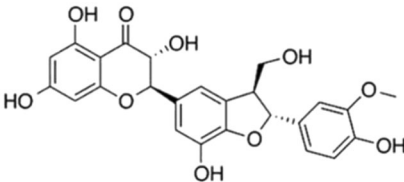
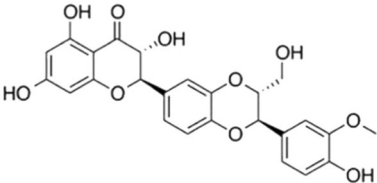
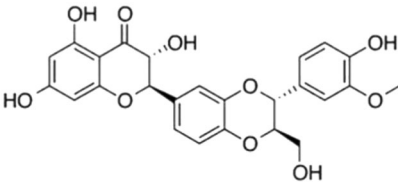
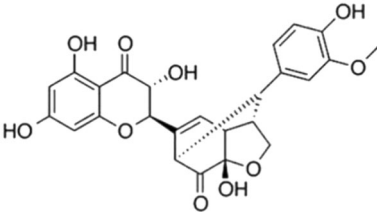
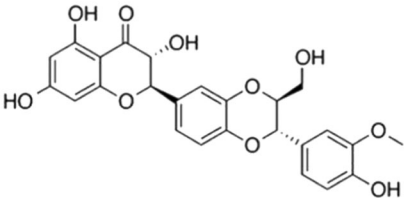
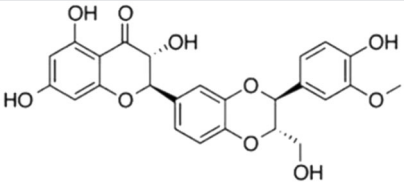
In this study, we conducted docking simulations to evaluate the interactions of the six compounds contained in the *S. marianum* extract

with the homology modeling structure of *hCA* VA. A threshold G-score of -4.48 kcal/mol, derived from the best docking pose of acetazolamide (AAZ) as a positive control on *hCA* VA, was established. Out of the six compounds, only two ligands exhibited G-scores lower than AAZ, suggesting their potential inhibitory activity against the target enzyme (Table 1). Specifically, silychristin and isosilybin A were identified as potential inhibitors of *hCA* VA, with G-scores of -4.63 and -4.53 kcal/mol, respectively. The complexes of silychristin and isosilybin A with *hCA* VA were further analyzed thermodynamically using the molecular mechanics/generalized Born surface area (MMGBSA) method.^[23] To assess their selectivity for the

mitochondrial isoform, we also analyzed their complexes with other *hCA* isoforms for which crystal structures are available in the PDB. Specifically, we compared the binding free energy values (ΔG_{bind}) of the two compounds from the *S. marianum* extract to those of the reference ligand AAZ, used as a positive control (Table 2).

The resulting data proved highly valuable in elucidating the key forces driving the interactions between the selected compounds and the *hCA* isoforms, providing insights into their underlying selectivity. Notably, our compounds exhibited better binding free energy (ΔG_{bind}) values compared with AAZ for both the *hCA* VA (the primary isoform of interest) and VII, an isoform involved in oxidative stress protection

TABLE 1 Pubchem ID (CID), common name, 2D structure, and G-Scores (kcal/mol) value for the six most abundant molecules in milk thistle extracts studied as potential *hCA* VA inhibitors.

Pubchem CID	Common name	2D Structure	G-Score (kcal/mol)
441764	Silychristin		-4.63
11059920	Isosilybin A		-4.53
31553	Silybin A		-4.44
11982272	Silidianin		-4.43
10885340	Isosilybin B		-4.08
1548994	Silybin B		-3.78

Note: Only silychristin and isosilybin A exceeded the cut-off value of the AAZ.

Abbreviation: AAZ, acetazolamide.

and neuropathic pain (Table 2).^[24,25] Specifically, silychristin and isosilybin A demonstrated ΔG_{bind} values of -27.02 and -28.53 kcal/mol, respectively, for *hCA* VA, and -48.35 and -41.77 kcal/mol for *hCA* VII. Conversely, these compounds showed lower affinity toward all other isoforms compared with AAZ, underscoring their potential selectivity for *hCA* VA and *hCA* VII.

Regarding the components related to ΔG_{bind} , in both *hCAs* isoforms complexes, we identified the lipophilic (ΔG_{Lipo}) and van der Waals (ΔG_{vdW}) contributions as the most significant for the two

TABLE 2 ΔG_{bind} values of silychristin and isosilybin A complexed with each *hCA* isoform.

<i>hCA</i> isoforms	Silychristin ΔG_{bind} (kcal/mol)	Isosilybin A ΔG_{bind} (kcal/mol)
<i>hCA</i> I	-41.00	-36.25
<i>hCA</i> II	-33.21	-33.16
<i>hCA</i> VA	-27.02	-28.53
<i>hCA</i> VII	-48.35	-41.77
<i>hCA</i> IX	-22.08	-21.37
<i>hCA</i> XII	-36.48	-39.04

Note: All ΔG values are reported in kcal/mol.

Abbreviation: *hCA*, human carbonic anhydrase.

compounds found in MT, compared with AAZ. The ΔG_{Lipo} values for silychristin and isosilybin A are very similar, at -14.82 and -14.79 kcal/mol, respectively, while the ΔG_{vdW} values are -38.08 and -39.72 kcal/mol, respectively. In comparison, the binding of AAZ to both *hCA* VA and *hCA* VII active sites is mainly influenced by electrostatic interactions, as evidenced by its more favorable ΔG_{Coul} values of -50.84 and -77.97 kcal/mol. Among the *hits*, isosilybin A exhibited a significant electrostatic contribution with a ΔG_{Coul} value of -32.32 kcal/mol when complexed with *hCA* VA. On the other hand, silychristin demonstrated an even greater electrostatic contribution with a ΔG_{Coul} value of -52.50 kcal/mol when complexed with *hCA* VII. By analyzing the solvation penalty, we observed the highest ΔG_{SolvGB} values for isosilybin A (49.93 kcal/mol) when complexed with *hCA* VA, and for AAZ (64.83 kcal/mol) when complexed with *hCA* VII.

By evaluating the docking poses, we observed distinct binding modes for both silychristin and isosilybin A in *hCA* VA and *hCA* VII (Figure 1 and Supporting Information S2: Figure S1). Specifically, in the best docking pose with the *hCA* VA, silychristin formed two π - π interactions: one between its hydroxyl-methoxyphenyl moiety and TYR 100, and another between its dihydrobenzofuran ring and HIS 130. Furthermore, the dihydrobenzofuran ring also participated in electrostatic interactions with the zinc ion (Figure 1a and Supporting Information S2: Figure S1A). Conversely, the docking analysis for the *hCA* VII active site revealed the formation of four hydrogen bonds

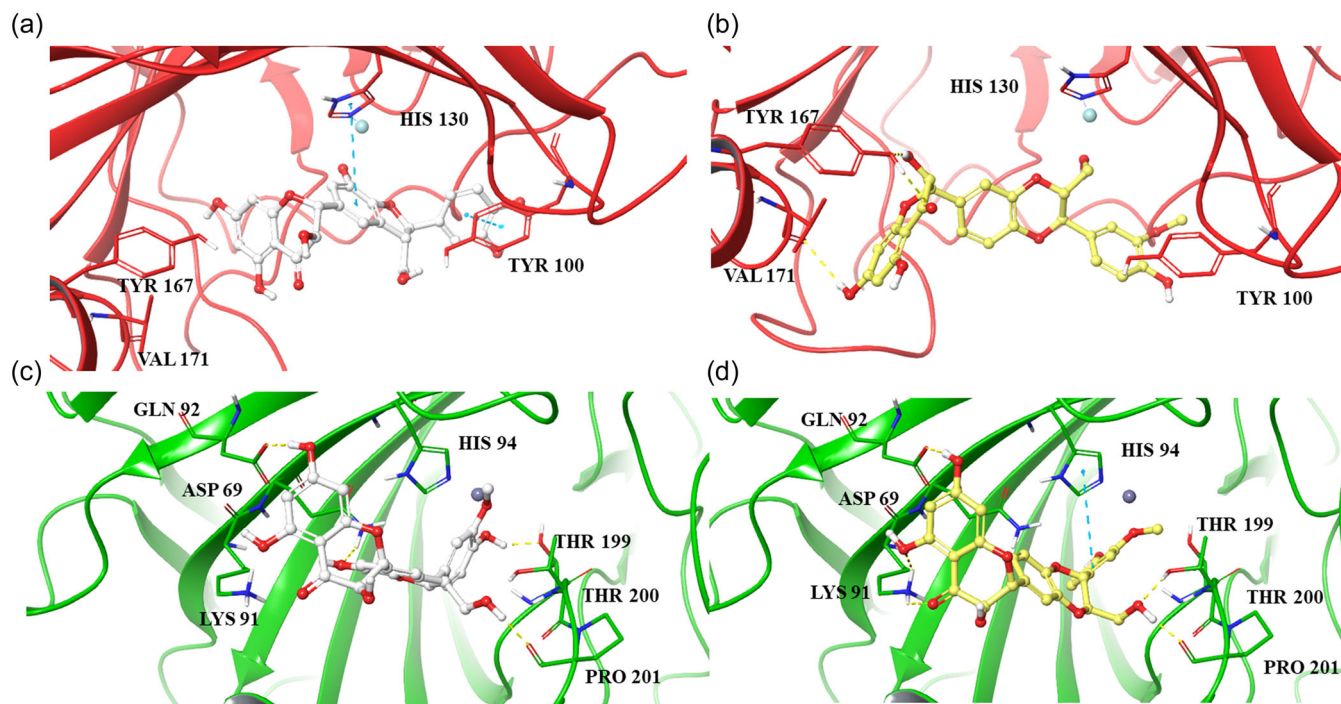


FIGURE 1 Three-dimensional (3D) representation of human carbonic anhydrase (*hCA*) VA and *hCA* VII complexed with (a, c) silychristin and (b, d) isosilybin A, respectively. Silychristin and isosilybin A are depicted as gray and yellow ball-and-stick models, while the zinc ion is shown as a gray sphere. *hCA* VA and *hCA* VII are represented as red and green cartoons, respectively. Additionally, the amino acid residues involved in the most significant interactions with the ligands are shown as red and green sticks for *hCA* VA and *hCA* VII, respectively. H-bonds, salt bridges, and stacking interactions are illustrated as yellow, red, and cyan dashed lines, respectively.

(H-bonds) involving the hydroxyl groups of the silychristin and the residues ASP 69, GLN 92, THR 199, and PRO 201. Additionally, its hydroxyl-methoxyphenyl moiety was oriented toward the zinc ion, facilitating potential electrostatic interactions (Figure 1b, Supporting Information S2: Figure S1B). For isosilybin A, the best docking pose with *hCA* VA revealed that the ligand was well-accommodated within the catalytic site, primarily stabilized by three hydrogen bonds (H-bonds) between the 2,3-dihydrochromen-4-one group and the residues TYR167 and VAL171. Furthermore, the 1,4-benzodioxine moiety formed favorable electrostatic interactions with the zinc ion (Figure 1c, Supporting Information S2: Figure S1C). On the other hand, in the *hCA* VII complex, docking analysis revealed a prominent cation- π interaction between the hydroxymethoxyphenyl group of isosilybin A and HIS94, along with two H-bonds with THR200 and PRO201, and two additional H-bonds with ASP69 and LYS91 through the dihydrocoumarin moiety (Figure 1d and Supporting Information S2: Figure S1D).

2.2 | MDs

MDs were performed to investigate the Induced-Fit (IF) process triggered by the binding of silychristin and isosilybin A to *hCA* VA and *hCA* VII, starting from their best docking poses. Compared with AAZ, the ligands extracted from *S. marianum* displayed similar behavior on both CA isoforms. This is evidenced by the comparable root mean square deviation (RMSD) values calculated for the protein-heavy atoms (Supporting Information S2: Figure S2A-B).

Regarding the RMSD trend calculated for the ligand-heavy atoms, both compounds demonstrated a rearrangement in their binding mode compared with AAZ (Supporting Information S2: Figure S2C-D). This observation suggests a more pronounced IF process for the ligands than for the protein. Specifically, isosilybin A showed an initial adjustment in both isoform complexes that persisted throughout the MDs (Supporting Information S2: Figure S2C-D, green line). Conversely, silychristin exhibited behavior similar to AAZ during the first 130 ns of MD simulations for the *hCA* VA complex (Supporting Information S2: Figure S2C, blue line), showing only minor changes toward the end. However, in the *hCA* VII complex, silychristin underwent significant alterations in its binding mode after 100 ns, reaching RMSD values of 6 Å (Supporting Information S2: Figure S2D, blue line). The higher RMSD values and greater fluctuations for isosilybin A and silychristine in both figures suggest a more dynamic interaction with the protein, undergoing significant conformational changes during the binding process. In contrast, AAZ's stable RMSD values indicate a more rigid and consistent binding mode, reflecting less structural adaptation in response to the protein environment. These data underscore the importance of considering the flexibility and IF potential of ligands in drug design and binding studies.

Finally, we conducted a detailed analysis of the interactions between the ligand atoms and the protein residues throughout the simulation (Figure 2). Specifically, our focus was on interactions that occurred for more than 30.0% of the total simulation time.

In our MD simulations involving *hCA* VA, we observed two distinct interaction patterns for our compounds, with the exception of the consistent electrostatic interaction between a hydroxyl group of both compounds and the zinc ion throughout the entire simulation (Figure 2a,b). Two notable interactions between silychristin and *hCA* VA occurred during 92% of the simulation time. These included a π - π interaction between the 2,3-dihydrobenzofuran moiety and HIS 130, and an H-bond formed between the phenolic group of the same moiety and GLU 142. Moreover, the hydroxychroman-4-one moiety engaged in two H-bonds with GLN 103, observed for 56% and 46% of the simulation, respectively, and formed a water bridge with THR 98 (Figure 2a). On the other hand, the binding mode of isosilybin A was defined by several water bridges with the residues SER 65, GLU 142, SER 233, and TRP 245, as well as hydrophobic interactions with TYR 100 and LEU 177 (Figure 2b). Despite the high RMSD trend for both compounds in *hCA* VII complex (Supporting Information S2: Figure S2D), silychristin and isosilybin A have strong and stable interactions within this binding pocket (Figure 2c,d). The ligands establish electrostatic interactions with the Zn^{2+} and form multiple H-bonds with high occupancy, indicating their significance in maintaining the binding conformation after the IF process. In particular, the MD simulations of the *hCA* VII complexes revealed persistent electrostatic interactions between the o-methoxy-phenolic portion of both compounds and the Zn^{2+} ion, maintained consistently throughout the entire simulation (Figure 2c,d). Specifically, the isosilybin A binding mode was characterized by different water bridges involving the residues ASP 69, THR 199, THR 200, and PRO 201, as well as an important H-bond with HIS 119 (Figure 2d). Similarly, silychristin maintained an H-bond with HIS 119 for almost 90% of the MD simulations. Additionally, its binding mode exhibited four other stable H-bonds with the residues GLN 92, ASP 69, THR 200, and PRO 201, along with a π - π interaction with HIS 94 (Figure 2c).

2.3 | Carbonic anhydrase inhibition assays

The inhibition profiles of silychristin and isosilybin A on the physiologically relevant *hCAs* I, II, VA, VII, IX, and XII were determined through the stopped-flow CO_2 hydrase assay^[26] and were compared with the commercially available AAZ as reference. Inhibition constants (K_i) were reported in Table 3.

As shown in Table 3, silychristin and isosilybin A were ineffective inhibitors on the broadly expressed *hCAs* I, II, and on the tumor-associated IX isoforms (K_i s > 100 μM). Conversely, close matching values were obtained for the central nervous system (CNS) related *hCA* VII as silychristin and isosilybin A have K_i values of 0.90 and 0.94 μM , respectively. Substantial kinetic discrimination was observed for the mitochondrial *hCA* VA, being the Isosilybin A 5.7-fold more effective inhibitor when compared with silychristin (i.e., K_i s of 5.25 and 0.92 μM for silychristin and isosilybin A, respectively). Medium micromolar values were obtained for both compounds on the *hCA* XII isoform (i.e., K_i s of 59.8 and 76.6 μM for silychristin and isosilybin A, respectively).

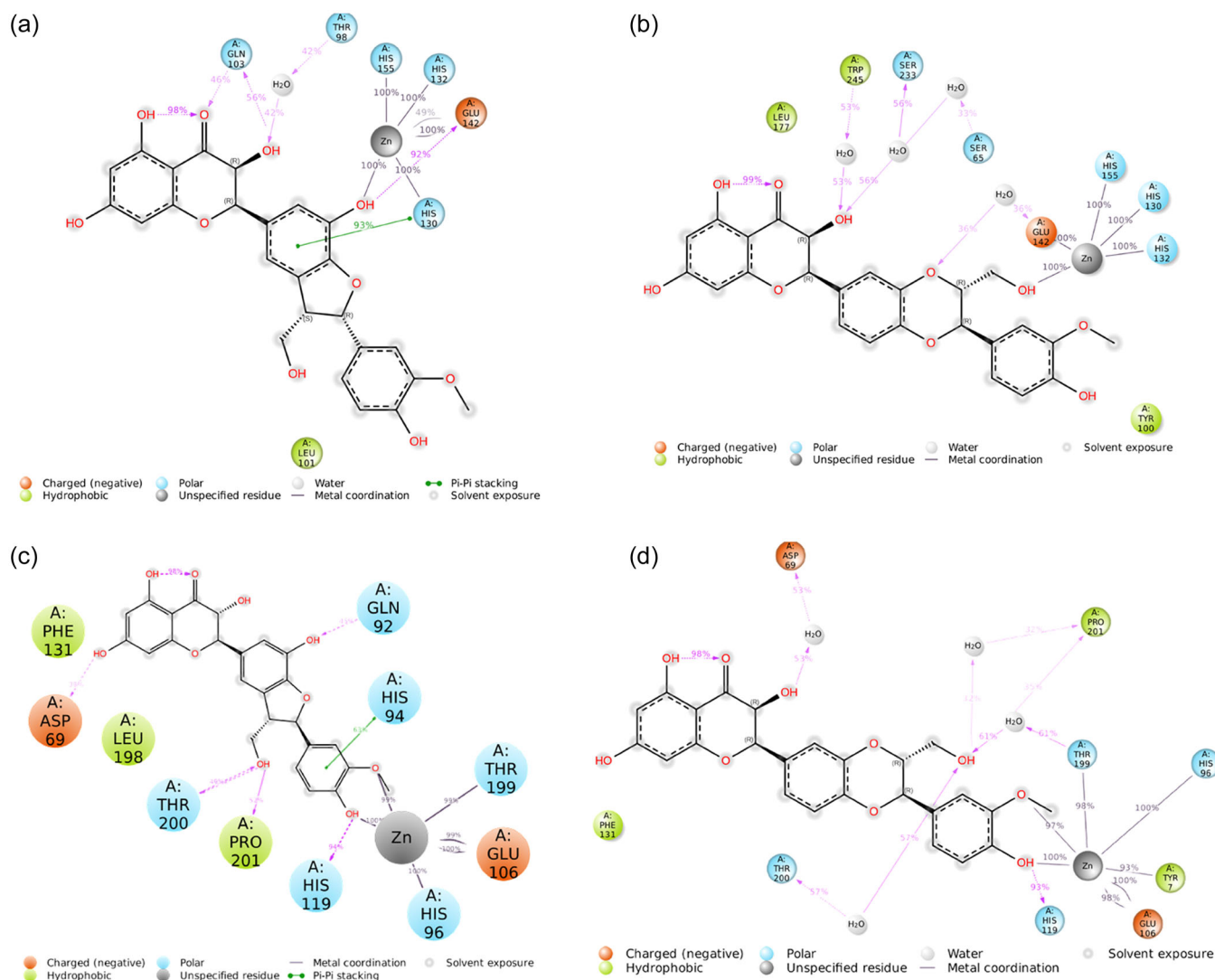


FIGURE 2 Ligand atom interactions with the human carbonic anhydrase (hCA) VA and hCA VII residues, for silychristin (a–c) and isosilybin A (b–d), respectively. Only interactions that occur more than 30.0% of the simulation time in 200 ns of the trajectory are shown.

TABLE 3 Inhibition data of silychristin and isosilybin A and the references AAZ on hCAs I, II, VA, VII, IX, and XII.^[26]

K_i (μM) ^a						
Compounds	hCA I	hCA II	hCA VA	hCA VII	hCA IX	hCA XII
Silychristin	>100	>100	5.25	0.90	>100	59.8
Isosilybin A	>100	>100	0.92	0.94	>100	76.6
AAZ	0.25	0.012	0.063	0.003	0.026	0.006

Abbreviation: AAZ, acetazolamide.

^aMean from 3 different assays by a stopped-flow technique. Errors were in the range of ± 5 –10% of the reported values.

In agreement with the predicted binding modes of silychristin and isosilybin A for the hCAs, the experimental *in vitro* inhibition potencies were far higher than the reference drug AAZ which possesses the prototypic CA inhibitory moiety of the primary

sulfonamide type. For instance, the hCA VA submicromolar inhibitor isosilybin A was 14.6-fold less effective when compared with AAZ (i.e., K_i of 0.063 μM), and such difference was up to 83.3-fold higher for silychristin when tested on the same enzyme. Data in Table 3 clearly showed that the high effectiveness of both natural products toward the hCA VII was not comparable to the reference AAZ, which exhibited a K_i of 3.0 nM. Even more drastic differences were reported for the tumor-associated hCA XII isoform as silychristin and Isosilybin A were 10.000- and 12.777-fold less effective when compared with AAZ (i.e. K_i s of 59.8, 76.6, and 0.006 μM , respectively).

It is, therefore, clear that silychristin is highly effective and selective for the hCA VII being the associated K_i value of 0.90 μM . The same potency was reported for isosilybin A, which is an equipotent inhibitor of both the hCAs VA and VII (K_i s of 0.92 and 0.94 μM for hCA VA and VII, respectively).

3 | CONCLUSION

The results of this study highlight the potential of two compounds from *S. marianum* (MT)—silychristin and isosilybin A—as selective inhibitors of specific *hCA* isoforms, particularly *hCA* VA and *hCA* VII. This conclusion is supported by an integrative approach combining docking simulations, MD simulations, and in vitro inhibition assays. The docking analysis suggests a potential affinity of these compounds for *hCA* VA, revealing a novel mechanism of action and positioning them as promising candidates for antiobesity pharmacology. The biophysical assays confirmed their inhibitory activity against *hCA* VA, reinforcing their potential as antiobesity agents. Computational studies further predicted the selectivity of silychristin and isosilybin A for *hCA* VA and VII, which was validated by the biophysical assays. Thermodynamic and interaction analyses showed that the inhibitory activity of these compounds is driven by a combination of lipophilic, Van der Waals, and electrostatic interactions, along with extensive hydrogen bonding. The lipophilic and Van der Waals forces were the primary contributors, providing significant stabilization in the binding sites of both *hCA* VA and VII. While AAZ exhibited stronger overall electrostatic interactions, silychristin, and isosilybin A formed extensive hydrogen bonding networks, particularly with residues around the zinc ion, as well as several water bridges, contributing to their stable and selective binding profiles.

Regarding the electrostatic interactions with the zinc ion observed in the best docking poses, it is important to note that the docking results may not fully match experimental literature data, partly due to the challenges of accurately modeling water molecules in the active site.^[27,28] Water molecules play a critical role in stabilizing ligand interactions, but their dynamic behavior is often oversimplified or overlooked in docking simulations.^[29] Additionally, because docking relies on molecular mechanics, it may not fully capture electronic effects such as polarization and charge transfer, which are better addressed through quantum mechanical methods.^[30] These limitations can lead to some variability in the predicted binding affinities and interaction profiles. Despite these limitations, docking remains a valuable and widely used tool for predicting ligand–enzyme interactions, providing rapid insights into binding poses, interaction patterns, and relative binding affinities. In this study, the docking results offer a strong foundation for understanding the key forces behind the inhibitory activity of the compounds and highlight their potential selectivity, which is further corroborated by complementary analyses like MDs simulations.^[31,32]

The selective inhibition of *hCA* VA and VII by silychristin and isosilybin A offers promising therapeutic opportunities, particularly for conditions associated with these isoforms. *hCA* VA plays a critical role in mitochondrial function, and its inhibition could have significant therapeutic potential for disorders linked to mitochondrial dysfunction, including neurodegenerative diseases, metabolic disorders, and age-related conditions. Targeting *hCA* VA, silychristin, and isosilybin A may provide a novel approach to mitigate symptoms or slow disease progression by enhancing mitochondrial efficiency and optimizing cellular energy production.

Similarly, *hCA* VII, predominantly expressed in the central nervous system (CNS), is involved in regulating oxidative stress, pain pathways, and neuroinflammation.^[24,33] Inhibition of *hCA* VII could be highly beneficial for conditions involving oxidative damage, neuropathic pain, and neurodegenerative diseases such as Alzheimer's, Parkinson's, and multiple sclerosis. The ability of silychristin and isosilybin A to selectively target *hCA* VII suggests that these compounds may offer a more targeted therapeutic strategy, potentially reducing the harmful effects of oxidative stress and neuroinflammation in the brain and spinal cord.^[24]

A key advantage of these compounds is their high selectivity for *hCA* VA and VII, which minimizes the risk of off-target effects commonly seen with nonselective carbonic anhydrase inhibitors. *hCAs* I, II, and IX are involved in a range of physiological processes, and nonselective inhibition of these isoforms can lead to adverse side effects, such as electrolyte imbalances, gastrointestinal issues, or cognitive disturbances. The lack of significant activity against these isoforms in silychristin and isosilybin A significantly lowers the risk of such complications, positioning these compounds as safer alternatives for therapeutic use. This selective inhibition not only enhances the therapeutic potential of these compounds but also underscores their specificity as promising drug candidates, with a reduced risk of unwanted side effects—an essential feature in the development of drugs for chronic and complex diseases.

This study highlights the promising potential of silychristin and isosilybin A as selective inhibitors of *hCA* VA and *hCA* VII, offering therapeutic promise for conditions linked to mitochondrial dysfunction and oxidative stress. The integrative approach, combining docking simulations, MD, and biophysical assays, has demonstrated the compounds' high selectivity and stable binding profiles, supporting their suitability for drug development. Finally, the lack of significant off-target effects, particularly on *hCA* isoforms I, II, and IX, strengthens the case for their use in treating chronic and complex diseases, making them strong candidates for further clinical investigation.

4 | EXPERIMENTAL

4.1 | Receptor preparation

Due to the unavailability of experimental structures of human carbonic anhydrase V (*hCA* V), we employed the homology model previously developed and validated in our study to advance our investigation into this isoform and its inhibitors.^[24] Additionally, we examined the interaction of the selected compounds with other isoforms to evaluate their selectivity for our target isoform. Thus, we obtained the crystallographic structure of various isoforms of *hCAs* from the Protein Data Bank (PDB).^[34] After careful consideration, we selected the models with the following PDB code for our analysis: 7QOD for *hCA* I,^[35] 6SBL for *hCA* II,^[36] 6SDT for *hCA* VII,^[37] 5FL4 for *hCA* IX,^[38] and 5MSA for *hCA* XII.^[39] The Protein Preparation Wizard tool^[40] to prepare the three-dimensional (3D) structures of all

the hCA isoforms, by applying OPLS3 as a force field.^[41] All models were refined for increased accuracy using the advanced Prime module to reconstruct missing side chains.^[42] Hydrogen atoms were added, and side-chain protonation states were assigned at pH 7.4. Any crystallographic buffer components and water molecules remaining in the model were removed. Subsequently, the co-crystallized ligands were set as centroids for generating the rigid receptor grid, which was defined by a $10 \times 10 \times 10$ Å inner box.

4.2 | Ligands preparation

From Pubchem,^[43] we downloaded the six CID (Chemical Identifier) of the most prevalent and biologically active compounds extracted from the *S. marianum* species. These six molecules were prepared using Ligprep at pH 7.4, maintaining default chirality.^[44] The molecules were minimized and optimized using the OPLS3 as a force field for subsequent docking studies. Acetazolamide (AAZ) was prepared using the same protocol and served as a positive control in this process.

4.3 | Docking simulations

For our docking simulations, we used Glide ver. 7.8 software applying the Standard-Precision (SP) protocol.^[45] We generated 10 poses for each ligand using default settings and selected the best binding mode based on the docking scoring function (G-Score). Thus, the re-docking analysis was performed for each PDB model to verify the reliability of our docking protocol for this model (Supporting Information S2: Table S1). First, we filtered the compounds with promising affinity for hCA V based on their G-score values. Specifically, we used the best G-score (−4.48 kcal/mol) obtained from the docking of AAZ with the hCA VA isoform as the cut-off (Supporting Information S2: Table S2). Compounds that successfully cleared the hCA V filter underwent evaluation on the remaining isoforms, with AAZ serving as the reference once more. Specifically, a thermodynamic analysis was performed on the best binding pose of the compounds across all isoforms. In fact, the MMGBSA method has been widely used in the study of protein–ligand interactions.^[46–49] Its application allowed the calculation of binding free energies (ΔG_{bind}) of the complexes of the selected compounds, providing valuable insight into their thermodynamic stability.

4.4 | MDs simulations

The best complexes of hCA VA and hCA VII with the two most promising compounds from *S. marianum* (silychristin and isosilybin A), as selected from docking, were submitted to 200 ns of MDs using Desmond ver. 4.4.^[50] All systems were enclosed within an orthorhombic box with a 10 Å thickness, containing the water solvent. Specifically, we employed the TIP3P water model parameters.^[51] The

charge of all systems was neutralized by adding Na^+ as counterions. We optimized the solvated model for accuracy and then relaxed it using the Martyna–Tobias–Klein isobaric-isothermal ensemble (MTK_NPT). Equilibration was ensured through both the NVT ensemble at 10 K and the NPT ensemble at 300 K and 1 atm with the Berendsen thermostat–barostat. Our analysis involved sampling trajectory frames every 200 ps and utilizing tools such as the Simulation Interaction Diagram and the Simulation Event Analysis. These tools facilitated a thorough exploration of the complex geometric and thermodynamic properties underlying the trajectories obtained. Additionally, we employed the same rigorous methodology to investigate both hCA isoforms complexes, alongside the well-established inhibitor AAZ, which had been utilized in the prior docking process. This comprehensive approach ensured the reliability and consistency of the findings across all systems studied.

4.5 | Carbonic anhydrase inhibition assays

An applied photophysics stopped-flow instrument was used to evaluate the ability of the test compounds to inhibit the CA-catalyzed CO_2 hydration.^[26] Phenol red (at a concentration of 0.2 mM) was used as an indicator, working at the absorbance maximum of 557 nm, with 20 mM 4-(2-hydroxyethyl)-1-piperazineethanesulfonic acid (pH 7.4) as a buffer, and 20 mM Na_2SO_4 (to maintain constant ionic strength), following the initial rates of the CA-catalyzed CO_2 hydration reaction for a period of 10–100 s. The CO_2 concentrations ranged from 1.7 to 17 mM for the assessment of the kinetic parameters and inhibition constants. Enzyme concentrations varied between 5 and 12 nM.^[52,53] For each inhibitor, at least six traces of the initial 5%–10% of the reaction were used to determine the initial velocity. The uncatalyzed rates were calculated in the same manner and subtracted from the total observed rates. Stock solutions of each inhibitor (0.1 mM) were prepared in distilled–deionized H_2O , and dilutions up to 0.01 nM were done thereafter with the assay buffer. Inhibitor and enzyme solutions were preincubated together for 15 min at room temperature before the assay, to allow for the formation of the E–I complex.^[53] The inhibition constants were obtained by nonlinear least-squares methods using PRISM 3^[26] and the Cheng–Prusoff equation as reported earlier^[54,55] and represent the mean from at least three different determinations. hCAs I and II were purchased from Merck, while hCAs IX and XII are recombinant and obtained in-house.^[56–60]

ACKNOWLEDGMENTS

This research was funded by PON “Ricerca e Innovazione” 2014–2020, grant number No. 26” code DOT13C5773-4. Francesco Fanelli, EVRA srl, Località Galdo Zona Industriale Lotto 2085044, Lauria (P. Z.). Open access publishing facilitated by Università degli Studi Magna Graecia di Catanzaro, as part of the Wiley - CRUI-CARE agreement.

CONFLICTS OF INTEREST STATEMENT

The authors declare no conflicts of interest.

DATA AVAILABILITY STATEMENT

Data that support the findings of this study are available in the supplementary material of this article.

ORCID

Roberta Rocca  <http://orcid.org/0000-0002-0680-7097>

Giosuè Costa  <http://orcid.org/0000-0003-0947-9479>

Gioele Renzi  <http://orcid.org/0009-0008-9109-030X>

Fabrizio Carta  <http://orcid.org/0000-0002-1141-6146>

Stefano Alcaro  <http://orcid.org/0000-0002-0437-358X>

REFERENCES

- [1] G. Twig, G. Yaniv, H. Levine, A. Leiba, N. Goldberger, E. Derazne, D. Ben-Ami Shor, D. Tzur, A. Afek, A. Shamiss, Z. Haklai, J. D. Kark, *N. Engl. J. Med.* **2016**, 374, 2430. <https://doi.org/10.1056/NEJMoa1503840>
- [2] E. E. Calle, *BMJ* **2007**, 335, 1107. <https://doi.org/10.1136/bmj.39384.472072.80>
- [3] H. Zhong, J. Dong, L. Zhu, J. Mao, Y. Zhao, Y. Zou, M. Guo, G. Ding, *Am. J. Transl. Res.* **2024**, 16, 387. <https://doi.org/10.62347/KMSA5983>
- [4] L. G. Bjerregaard, B. W. Jensen, L. Ångquist, M. Osler, T. I. A. Sørensen, J. L. Baker, *N. Engl. J. Med.* **2018**, 378, 1302. <https://doi.org/10.1056/NEJMoa1713231>
- [5] T. D. Müller, M. Blüher, M. H. Tschöp, R. D. DiMarchi, *Nat. Rev. Drug Discovery* **2022**, 21, 201. <https://doi.org/10.1038/s41573-021-00337-8>
- [6] GBD 2015 Obesity Collaborators, *N. Engl. J. Med.* **2017**, 377, 13. <https://doi.org/10.1056/NEJMoa1614362>
- [7] L. M. S. Carlsson, K. Sjöholm, P. Jacobson, J. C. Andersson-Assarsson, P. A. Svensson, M. Taube, B. Carlsson, M. Peltonen, *N. Engl. J. Med.* **2020**, 383, 1535. <https://doi.org/10.1056/NEJMoa2002449>
- [8] A. Aspatwar, C. T. Supuran, A. Waheed, W. S. Sly, S. Parkkila, *J. Physiol.* **2023**, 601, 257. <https://doi.org/10.1113/JP283579>
- [9] C. T. Supuran, *J. Enzyme Inhib. Med. Chem.* **2022**, 37, 2478. <https://doi.org/10.1080/14756366.2022.2121393>
- [10] C. T. Supuran, G. De Simone, in *Carbonic Anhydrases as Biocatalysts: From Theory to Medical and Industrial Applications*, Elsevier, The Netherlands **2015**.
- [11] C. T. Supuran, A. Nocentini A, in *Carbonic Anhydrases: Biochemistry and Pharmacology of an Evergreen Pharmaceutical Target*, **2019**.
- [12] M. Balaji, M. S. Ganjavi, G. E. N. Hanuma Kumar, B. N. Parim, R. Mopuri, S. Dasari, *Obes. Res. Clin. Pract.* **2016**, 10, 363. <https://doi.org/10.1016/j.orcp.2015.12.004>
- [13] C. Ceccanti, M. Landi, S. Benvenuti, A. Pardossi, L. Guidi, *Molecules* **2018**, 23, 2299. <https://doi.org/10.3390/molecules23092299>
- [14] M. Marrelli, G. Statti, F. Conforti, *Molecules* **2020**, 25, 649. <https://doi.org/10.3390/molecules25030649>
- [15] A. Tajmohammadi, B. M. Razavi, H. Hosseinzadeh, *Phytother. Res.* **2018**, 32, 1933. <https://doi.org/10.1002/ptr.6153>
- [16] E. Köksal, I. Gülçin, S. Beyza, Ö. Sarikaya, E. Bursal, *J. Enzyme Inhib. Med. Chem.* **2009**, 24, 395. <https://doi.org/10.1080/14756360802188081>
- [17] D. Csupor, A. Csorba, J. Hohmann, *J. Pharm. Biomed. Anal.* **2016**, 130, 301. <https://doi.org/10.1016/j.jpba.2016.05.034>
- [18] C. S. Chambers, V. Holečková, L. Petrásková, D. Biedermann, K. Valentová, M. Buchta, V. Křen, *Food Res. Int.* **2017**, 100, 339. <https://doi.org/10.1016/j.foodres.2017.07.017>
- [19] L. Abenavoli, A. A. Izzo, N. Milić, C. Cicala, A. Santini, R. Capasso, *Phytother. Res.* **2018**, 32, 2202. <https://doi.org/10.1002/ptr.6171>
- [20] I. Marmouzi, A. Bouyahya, S. M. Ezzat, M. El Jemli, M. Kharbach, *J. Ethnopharmacol.* **2021**, 265, 113303. <https://doi.org/10.1016/j.jep.2020.113303>
- [21] A. Kołota, D. Głabska, *Appl. Sci.* **2021**, 11, 5836.
- [22] Y. Guo, S. Wang, Y. Wang, T. Zhu, *Pharm. Biol.* **2016**, 54, 2995. <https://doi.org/10.1080/13880209.2016.1199042>
- [23] H. Sun, L. Duan, F. Chen, H. Liu, Z. Wang, P. Pan, F. Zhu, J. Z. H. Zhang, T. Hou, *Phys. Chem. Chem. Phys.* **2018**, 20, 14450. <https://doi.org/10.1039/c7cp07623a>
- [24] R. Del Giudice, D. M. Monti, E. Truppo, A. Arciello, C. T. Supuran, G. De Simone, S. M. Monti, *Biol. Chem.* **2013**, 394, 1343. <https://doi.org/10.1515/hsz-2013-0204>
- [25] Ö. Akgül, E. Lucarini, L. Di Cesare Mannelli, C. Ghelardini, K. D'Ambrosio, M. Buonanno, S. M. Monti, G. De Simone, A. Angeli, C. T. Supuran, F. Carta, *Eur. J. Med. Chem.* **2022**, 227, 113956. <https://doi.org/10.1016/j.ejmech.2021.113956>
- [26] R. G. Khalifah, *J. Biol. Chem.* **1971**, 246, 2561. [https://doi.org/10.1016/S0021-9258\(18\)62326-9](https://doi.org/10.1016/S0021-9258(18)62326-9)
- [27] G. Costa, F. Carta, F. A. Ambrosio, A. Artese, F. Ortuso, F. Moraca, R. Rocca, I. Romeo, A. Lupia, A. Maruca, D. Bagetta, R. Catalano, D. Vullo, S. Alcaro, C. T. Supuran, *Eur. J. Med. Chem.* **2019**, 181, 111565. <https://doi.org/10.1016/j.ejmech.2019.111565>
- [28] A. Scozzafava, M. Passaponti, C. T. Supuran, I. Gülçin, *J. Enzyme Inhib. Med. Chem.* **2015**, 30, 586. <https://doi.org/10.3109/14756366.2014.956310>
- [29] M. Gidaro, F. Alcaro, S. Carradori, G. Costa, D. Vullo, C. Supuran, S. Alcaro, *Planta Med.* **2015**, 81, E1. <https://doi.org/10.1055/s-0034-1396263>
- [30] F. Stanzione, I. Giangreco, J. C. Cole, *Prog. Med. Chem.* **2021**, 60, 273. <https://doi.org/10.1016/bs.pmch.2021.01.004>
- [31] P. C. Agu, C. A. Afiukwa, O. U. Orji, E. M. Ezeh, I. H. Ofoke, C. O. Ogbu, E. I. Ugwuja, P. M. Aja, *Sci. Rep.* **2023**, 13, 13398. <https://doi.org/10.1038/s41598-023-40160-2>
- [32] W. Yu, A. D. MacKerell, *Methods Mol. Biol.* **2017**, 1520, 85. https://doi.org/10.1007/978-1-4939-6634-9_5
- [33] H. E. Duran, Ş. Beydemir, *Biotechnol. Appl. Biochem.* **2023**, 70, 415. <https://doi.org/10.1002/bab.2367>
- [34] S. K. Burley, C. Bhikadiya, C. Bi, S. Bittrich, L. Chen, G. V. Crichlow, C. H. Christie, K. Dalenberg, L. Di Costanzo, J. M. Duarte, S. Dutta, Z. Feng, S. Ganesan, D. S. Goodsell, S. Ghosh, R. K. Green, V. Guranović, D. Guzenko, B. P. Hudson, C. Lawson, Y. Liang, R. Lowe, H. Namkoong, E. Peisach, I. Persikova, C. Randle, A. Rose, Y. Rose, A. Sali, J. Segura, M. Sekharan, C. Shao, Y. P. Tao, M. Voigt, J. Westbrook, J. Y. Young, C. Zardecki, M. Zhuravleva, *Nucleic Acids Res.* **2021**, 49, D437. <https://doi.org/10.1093/nar/gkaa1038>
- [35] A. Zubrienė, A. Smirnov, V. Dudutienė, D. D. Timm, J. Matulienė, V. Michailovienė, A. Zakauskas, E. Manakova, S. Gražulis, D. Matulis, *ChemMedChem* **2017**, 12, 161. <https://doi.org/10.1002/cmdc.201600509>
- [36] S. Glöckner, K. Ngo, B. Wagner, A. Heine, G. Klebe, *Biomolecules* **2020**, 10, 509. <https://doi.org/10.3390/biom10040509>
- [37] A. Nocentini, V. Alterio, S. Bua, L. Micheli, D. Esposito, M. Buonanno, G. Bartolucci, S. M. Osman, Z. A. ALOthman, R. Cirilli, M. Pierini, S. M. Monti, L. Di Cesare Mannelli, P. Gratteri, C. Ghelardini, G. De Simone, C. T. Supuran, *J. Med. Chem.* **2020**, 63, 5185. <https://doi.org/10.1021/acs.jmedchem.9b02135>
- [38] J. Leitans, A. Kazaks, A. Balode, J. Ivanova, R. Zalubovskis, C. T. Supuran, K. Tars, *J. Med. Chem.* **2015**, 58, 9004. <https://doi.org/10.1021/acs.jmedchem.5b01343>
- [39] A. Smirnov, E. Manakova, S. Gražulis, D. Matulis, V. Dudutienė, *Crystal Structure of Human Carbonic Anhydrase Isozyme XII With 2, 3, 5, 6-Tetrafluoro-4-(Propylthio) Benzenesulfonamide*. Protein Data Bank. <https://doi.org/10.2210/pdb5msa/pdb> **2018**.
- [40] Schrödinger Release 2018-4: Protein Preparation Wizard. Epik, Schrödinger, LLC: New York, NY, USA. **2018**.
- [41] E. Harder, W. Damm, J. Maple, C. Wu, M. Reboul, J. Y. Xiang, L. Wang, D. Lupyan, M. K. Dahlgren, J. L. Knight, J. W. Kaus, D. S. Cerutti,

- G. Krilov, W. L. Jorgensen, R. Abel, R. A. Friesner, *J. Chem. Theory Comput.* **2016**, 12, 281. <https://doi.org/10.1021/acs.jctc.5b00864>
- [42] Schrödinger, *Prime*, Schrödinger, LLC, New York, NY, USA **2018**.
- [43] <https://pubchem.ncbi.nlm.nih.gov>.
- [44] Schrödinger, *LigPrep*, Schrödinger, LLC, New York, NY, USA **2018**.
- [45] Schrödinger, *Glide*, Schrödinger, LLC, New York, NY, USA **2018**.
- [46] F. Mesiti, A. Maruca, V. Silva, R. Rocca, C. Fernandes, F. Remião, E. Uriarte, S. Alcaro, A. Gaspar, F. Borges, *Eur. J. Med. Chem.* **2021**, 213, 113183. <https://doi.org/10.1016/j.ejmech.2021.113183>
- [47] G. Gualtieri, A. Maruca, R. Rocca, F. Carta, E. Berrino, A. Salatino, C. Brescia, R. Torcasio, M. Crispo, F. Trapasso, S. Alcaro, C. T. Supuran, G. Costa, *Antioxidants* **2023**, 12, 1115. <https://doi.org/10.3390/antiox12051115>
- [48] M. Barreca, V. Spanò, R. Rocca, R. Bivacqua, A. C. Abel, A. Maruca, A. Montalbano, M. V. Raimondi, C. Tarantelli, E. Gaudio, L. Cascione, A. Rinaldi, R. Bai, M. O. Steinmetz, A. E. Prota, S. Alcaro, E. Hamel, F. Bertoni, P. Barraja, *Eur. J. Med. Chem.* **2022**, 243, 114744. <https://doi.org/10.1016/j.ejmech.2022.114744>
- [49] R. Catalano, R. Rocca, G. Juli, G. Costa, A. Maruca, A. Artese, D. Caracciolo, P. Tagliaferri, S. Alcaro, P. Tassone, N. Amodio, *Eur. J. Med. Chem.* **2019**, 183, 111715. <https://doi.org/10.1016/j.ejmech.2019.111715>
- [50] Desmond Molecular Dynamics System, D. E. Shaw Research, New York, NY, **2018**.
- [51] D. Nayar, M. Agarwal, C. Chakravarty, *J. Chem. Theory Comput.* **2011**, 7, 3354. <https://doi.org/10.1021/ct2002732>
- [52] I. D'Agostino, G. E. Mathew, P. Angelini, R. Venanzoni, G. Angeles Flores, A. Angeli, S. Carradori, B. Marinacci, L. Menghini, M. A. Abdelgawad, M. M. Ghoneim, B. Mathew, C. T. Supuran, *J. Enzyme Inhib. Med. Chem.* **2022**, 37, 986. <https://doi.org/10.1080/14756366.2022.2055009>
- [53] D. Vullo, M. Durante, F. S. Di Leva, S. Cosconati, E. Masini, A. Scozzafava, E. Novellino, C. T. Supuran, F. Carta, *J. Med. Chem.* **2016**, 59, 5857. <https://doi.org/10.1021/acs.jmedchem.6b00462>
- [54] GraphPad Prism. www.graphpad.com (accessed: April 2024).
- [55] C. Yung-Chi, W. H. Prusoff, *Biochem. Pharmacol.* **1973**, 22, 3099. [https://doi.org/10.1016/0006-2952\(73\)90196-2](https://doi.org/10.1016/0006-2952(73)90196-2)
- [56] A. Angeli, I. Chelli, L. Lucarini, S. Sgambellone, S. Marri, S. Villano, M. Ferraroni, V. De Luca, C. Capasso, F. Carta, C. T. Supuran, *J. Med. Chem.* **2024**, 67, 3066. <https://doi.org/10.1021/acs.jmedchem.3c02254>
- [57] S. Haapanen, H. Barker, F. Carta, C. T. Supuran, S. Parkkila, *J. Med. Chem.* **2024**, 67, 152. <https://doi.org/10.1021/acs.jmedchem.3c01020>
- [58] A. Angeli, M. Ferraroni, C. Granchi, F. Minutolo, X. Chen, P. Shriwas, E. Russo, A. Leo, S. Selleri, F. Carta, C. T. Supuran, *J. Med. Chem.* **2023**, 66, 10010. <https://doi.org/10.1021/acs.jmedchem.3c00938>
- [59] G. Benito, I. D'Agostino, S. Carradori, M. Fantacuzzi, M. Agamennone, V. Puca, R. Grande, C. Capasso, F. Carta, C. T. Supuran, *Future Med. Chem.* **2023**, 15, 1865. <https://doi.org/10.4155/fmc-2023-0208>
- [60] I. D'Agostino, S. Zara, S. Carradori, V. De Luca, C. Capasso, C. H. M. Kocken, A. M. Zeeman, A. Angeli, F. Carta, C. T. Supuran, *ChemMedChem* **2023**, 18, e202300267. <https://doi.org/10.1002/cmdc.202300267>

SUPPORTING INFORMATION

Additional supporting information can be found online in the Supporting Information section at the end of this article.

How to cite this article: E. L. Citriniti, R. Rocca, G. Costa, G. Renzi, F. Carta, C. T. Supuran, S. Alcaro, F. Ortuso, *Arch. Pharm.* **2025**358:, e2400966. <https://doi.org/10.1002/ardp.202400966>